

Lasers in FEL Facilities

M. Divall

PSI, Villigen, Switzerland

Abstract

This paper gives an overview about where and how conventional lasers are used in Free-Electron Laser (FEL) facilities, covering lasers utilized for timing system distribution, electron injection, beam treatment and diagnostics, as well as in experimental stations. It starts with a short introduction to the necessary laser terminology. The required laser parameters for each application are shown, especially highlighting the specifications, which are state-of-the-art. Examples from FEL facilities are listed. Finally, the future for the building of compact FELs is discussed.

Keywords

Lasers; optical timing distribution; photo-injector; pump-probe experiments.

1 Introduction to lasers in layman's terms

In this section I focus on the basic building blocks of the laser system. The aim is to give a pointer towards the choices made in the scope of a Free-Electron Laser (FEL). More details can be found about lasers in general in [1].

A laser is a device that emits light through a process of optical amplification based on the stimulated emission of electromagnetic radiation. The term 'laser' originated as an acronym for 'light amplification by stimulated emission of radiation' [2]. The main difference between a conventional laser and a free-electron laser is that, in the former, electron are bound into the structure of a material, a lasing medium; while in the FEL the 'lasing medium' consists of very-high-speed electrons moving freely through a magnetic structure, and hence they are free. In the former the lasing properties will be determined by the material and its energy levels and other physical properties, while in the FEL, by the properties of the incoming electrons and the magnetic field structure they encounter.

Einstein postulated that photons prefer to travel together in the same state [3]. If one has a large collection of atoms containing a great deal of excess energy or, so to say, in an excited state, they will randomly emit a photon. If a photon of the correct wavelength passes through this excited material, its presence will stimulate the atoms to release their photons early – and those photons will travel in the same direction with the identical frequency and phase as the original stray photon. A cascading effect will start where these identical photons move through the rest of the material. As a result, ever more photons will be emitted from their atoms to join them, and an amplification process will take place. The observation was intuitive, but proven to be correct. This is a bit like announcing an FEL School and hence exciting likeminded people to gather together in the same place at the same time. May great things come out of such events.

1.1 The choice of the laser material

The choice of the laser material is determined by many different parameters. We would like our laser to emit at a specific wavelength and therefore we look for materials with a given emission band. This will automatically bring an absorption band, where we would like to find a matching pump source, which will bring our material to an excited state in the most efficient way, as shown in Fig. 1.

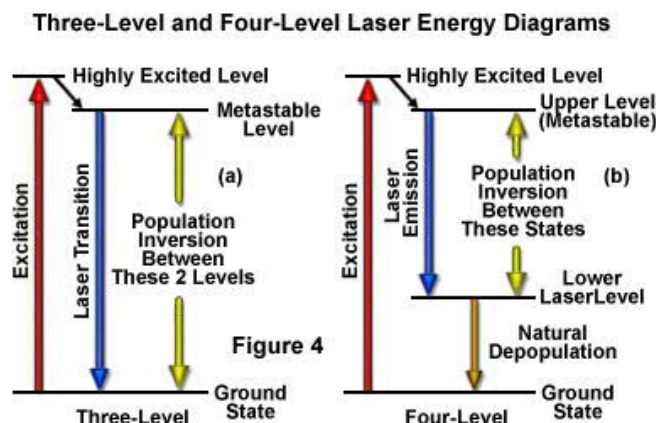


Fig. 1: The process of excitation and stimulated emission in (a) three-level systems; and (b) four-level systems [4]

The pulse shape and length and rise time are important for low emittance machines for FEL. When producing ultra-short laser pulses, below 100 fs, ultra-broadband emission is required, where the choice of materials is limited. Often, a second laser source is required for pumping. As in most cases a solid crystal material is used for such applications, we will limit ourselves to solid-state lasers. Some FELs, such as the European XFEL, generate a long train of electron bunches that are induced by the laser. Here, the fluorescence lifetime of the upper laser level will limit the length of the train, which can be produced with identical laser parameters. The stimulated emission cross-section and the gain properties of the material will determine the necessary amplification stages and hence the complexity of the laser system. The thermal properties of the crystal will determine the scalability of the system to high average powers as well as the quality of the beam.

As in FELs, synchronizability to the RF accelerating structures is required: the laser system starts with a laser cavity, called the oscillator. The repetition rate will limit the available materials as well as the pulse energy, often calling for several stages of amplification. The so-called saturation fluence determines how much energy can be extracted from a given volume of the material. Hence, the available crystal sizes and their thermal fracture limit will determine the maximum fluence that can be extracted efficiently from a single amplification stage. The difference between the pump and the emission band determines the proportion of the power converted into thermal losses, and will limit the average power or complicate the cooling system requirements.

Table 1 shows for the properties of the three most typically used materials for solid-state lasers, highlighting the parameters where a material excels compared to the others [5].

Table 1: Examples of the different amplifier materials and their properties

	Crystals		
	Nd:YAG	Yb:YAG	Ti:Saph
Fluorescence lifetime [ms]	0.23	0.96	0.0032
Stimulated-emission cross-section [$\times 10^{-20} \text{ cm}^{-1}$]	20 to 30	2.1	30
Lasing wavelengths [nm]	1064	1030	660 to 1100
Absorption wavelengths [nm]	808	941	514 to 532
Fluorescence bands (FWHM) [nm]	0.67	to 10	440
Absorption bands (FWHM) [nm]	1.9	>10	200
Pumping quantum efficiency	0.76	0.91	0.55
Saturation fluence [J/cm^2]	0.67	9.2	0.9

For picosecond pulse generation the materials most used are neodymium-doped, such as Nd:YLF, Nd:YVO₄ and Nd:YAG. The advantage of these materials is that the upper laser level lifetime is relatively long, in the hundreds of microsecond range, which allows for efficient energy storage, as well

as extraction of high repetition rate pulse trains, as opposed to single pulse generation. Furthermore, these materials can be pumped directly with diodes at ~ 800 nm. These diodes are available relatively cheaply, and also in stacks, which brings down the overall cost of the amplifiers.

For femtosecond pulse generation the most widely known material is titanium sapphire (Ti:Saph). The amplification bandwidth of this material allows for sub-10 fs pulse generation, which can be further amplified from the tens of millijoule level to sub-100 fs, and it is readily available on the market. The large bandwidth allows for manipulation of the pulse shape, which is often required for low emittance sources. The drawback is that it is not suitable for long pulse trains due to the short fluorescence lifetime. The absorption band (~ 500 nm) also falls outside the widely available pump diodes' range and therefore frequency-doubled Nd:YAG lasers are used to pump these systems, which increases cost and complexity.

Lasers based on ytterbium-doped materials (Yb:YAG, Yb:KGW, Yb:glass) provide a good compromise. They allow for sub-picosecond pulses and diode pumping, as well as for fibre-based oscillators and pre-amplifiers, making the system more robust and simple. Since a part for the system could be in fibre, the beam profile is also improved substantially.

The pumping source to achieve excitation of the upper laser level can vary, depending on the crystal geometry, the wavelength of absorption and the required repetition rate. Pumping by diodes is by far the most efficient and cost-effective solution. Diodes in the 800 nm to 950 nm range are readily available in diode-stack options, providing 1 kW/cm^2 mean power up to kilohertz repetition rates. The lifetime is estimated to be $\sim 10^9$ shots, which for a 100 Hz system would provide half a year of non-stop operation. When power is reduced to below nominal, the lifetime could be further extended. Flash-lamps are cheaper, but only provide a few weeks of operation at 100 Hz, and constant degradation often leads to other laser parameters changing between maintenance. When other lasers are used for pumping the main amplifier chain it can lead to very high energy broadband systems, but at the cost of inefficiency and complexity.

So the material is chosen after taking into consideration the pulse length, pulse structure, wavelength and maximum pulse energy required. In most cases a compromise needs to be taken between flexibility and robustness. As much of the system as possible should be acquired commercially, from industrial sources.

1.2 The architecture of the laser

The first element of a laser-chain is the oscillator. The oscillator has to provide the proper input wavelength for the rest of the amplifier chain, and the active material is often chosen to be the same as that of the amplifiers.

Figure 2 shows a schematic for an oscillator, containing a continuously pumped gain medium as well as a pulse-shortening and mode-locking device. What is unique to applications in FELs is that the laser pulses have to arrive synchronized at the RF accelerating cavities; the injector is synchronized to the electron bunches for the diagnostics, and to the FEL pulses at the experiments. This requires specific frequencies for the oscillator as well as an actively stabilized cavity to maintain the timing. The specific macro-pulse structure will also have an influence on the repetition rate.

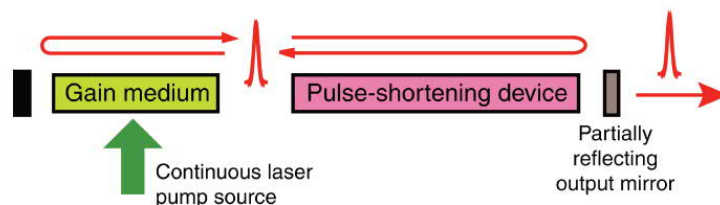


Fig. 2: Schematic of an oscillator (<http://slideplayer.com/slide/5110070> slide 6)

The pulses that are not needed in the machine are discarded, using acousto- or electro-optical switches, and the pulses are then further amplified. Figure 3(a) shows an example for the cavity design of a Ti:Saph laser, pumped by an external laser source and complex architecture to maintain the broad bandwidth, providing pulses in the tens of femtoseconds range, commercially available. In contrast Fig. 3 (b) illustrates the simplicity of a diode pumped Yb fibre oscillator [6], providing unmatched high power 10 ps pulses directly from the oscillator. For synchronization purposes at the 10s of fs level the pump-laser power noise, the mechanical stability, straight-light and electrical noise can all have an effect.

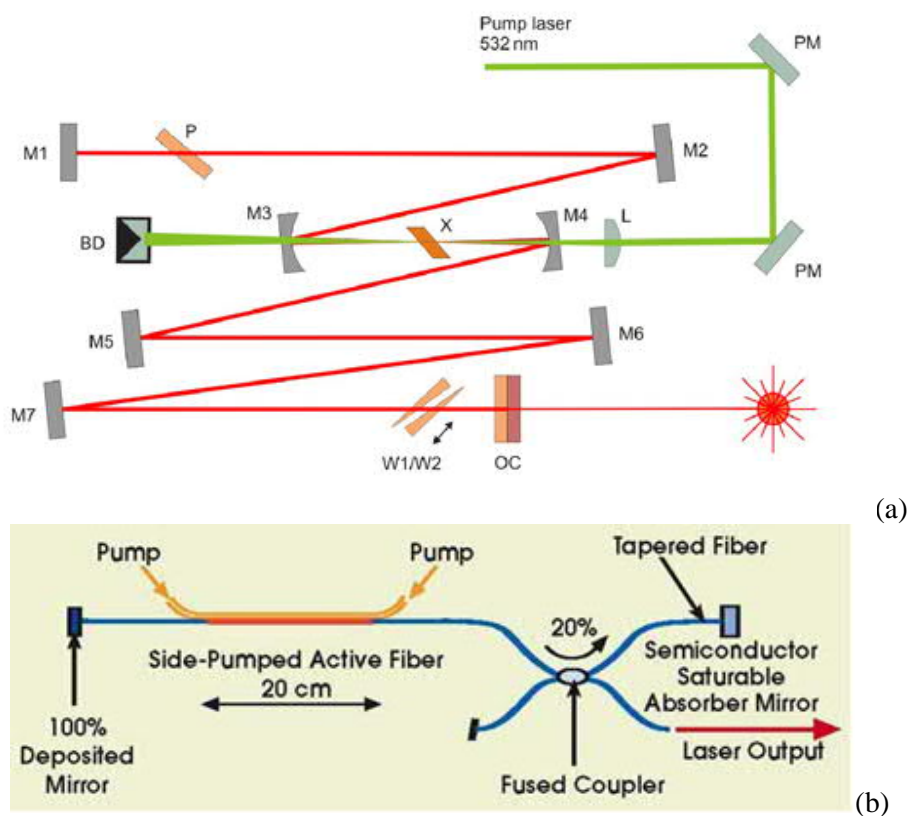


Fig. 3: Example of a (a) 4 fs Ti:Saph oscillator (<http://www.iqo.uni-hannover.de/591.html>); (b) ytterbium fibre laser.

As the non-linearities limit the energy that can be reached directly in an oscillator, the pulse energy below nanojoule level will require further amplification. The amplification can take place in different architectures. Figure 4(a) shows a multi-pass amplifier, most typically used for pre-amplification and the final amplifier stages. This arrangement makes it possible to amplify several pulses or pulse trains. The regenerative amplifier shown in Fig. 5(b) is recirculating a single pulse inside the amplifier, allowing for high gain and efficiency, but is only suitable for single pulse amplification.

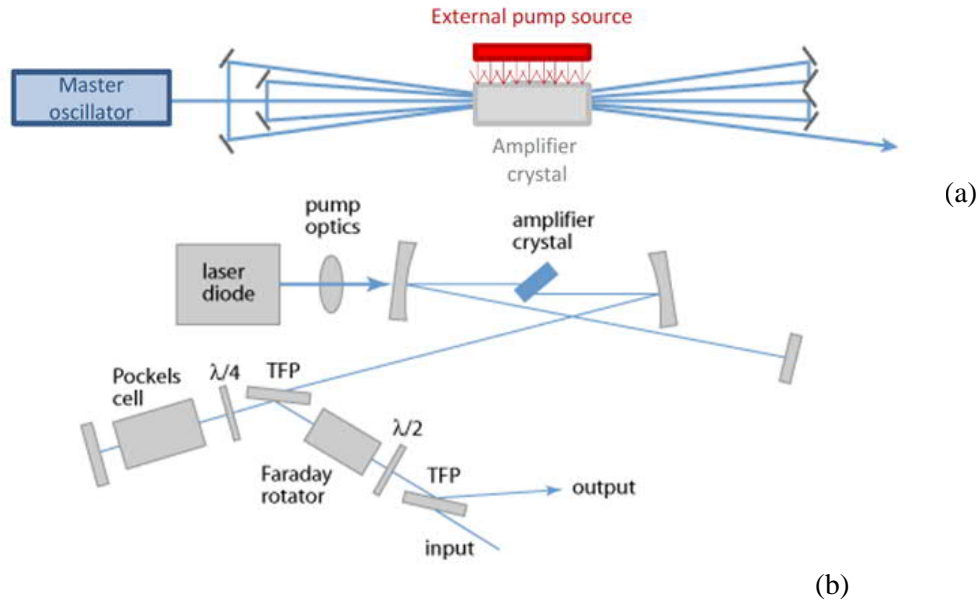


Fig. 4: (a) Multi-pass amplification; (b) regenerative amplifier

All of these amplifier types can be combined with the so-called chirped pulse amplification (CPA), shown in Fig. 5. To avoid damage in the amplifier due to the high peak intensity in a single short pulse, the laser pulse is stretched after the oscillator or pre-amplifier stage and only compressed again after the required energy is reached [7, 8].

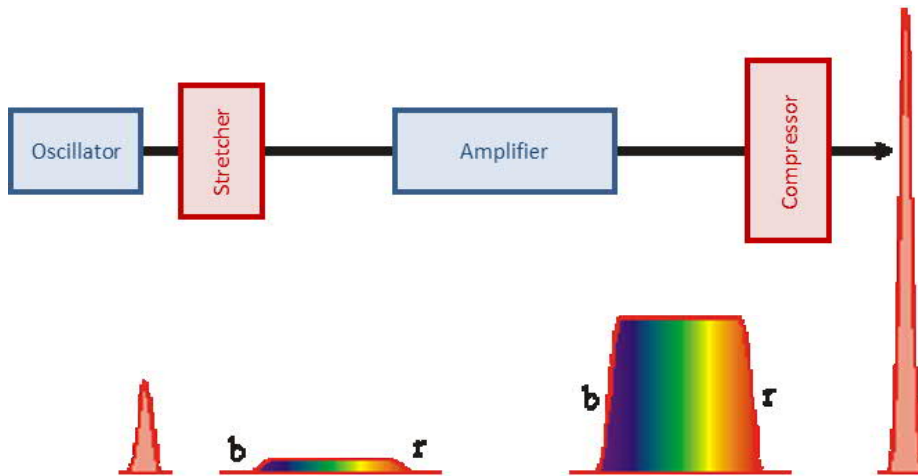


Fig. 5: Basic layout of a chirped pulse amplifier (CPA)

This is possible due to the high bandwidth of the laser, which allows for controlled spectral dispersion, or chirp. These types of amplifiers are able to reach Travelling Wave (TW) levels in a standard Ti:Saph system. The mechanical design of these systems is very important, as are the total amplification path and the alignment through the stretcher and the compressor. Another term needs to be clarified at this point. The layout of a so-called master oscillator power amplifier is shown in Fig. 6. There are an increasing number of FELs where the aim is to provide several pulses in a train, with the same properties. They should therefore be able to distribute FEL pulses between experiments, as well as sample processes that are on the timescale of the laser pulse train.

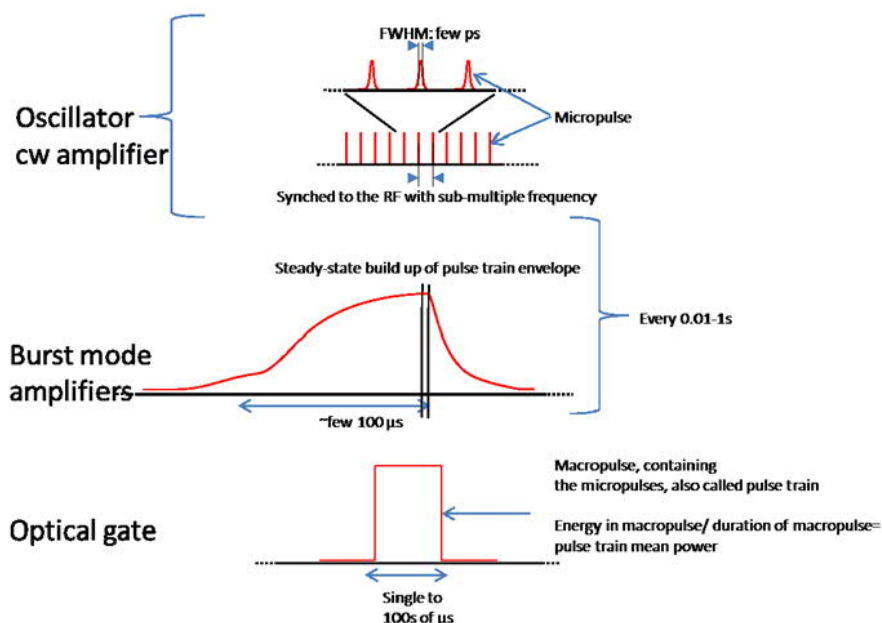


Fig. 6: Master oscillator power amplifiers for burst mode operation

In principle, oscillators allow for GHz pulse-train generation, but this often results in an extremely low energy single pulse at the front end of the system, making it difficult to maintain constant pulse characteristics throughout the amplification process. Master oscillator power amplifiers typically use a pulse train in the 100 MHz to 250 MHz repetition rate region. The pulse train is selected at the beginning of the amplification process. The amplifiers are operated in a burst mode and the train, containing pulses with identical parameters, is selected at the end. Thermal management of such systems can be difficult.

Last, but not least, we need to mention optical parametric amplifiers (OPA). These types of lasers are just becoming commercially available with the new European projects, such as ELI. Here the amplification takes place in a non-linear optical material, using a parametric process. The energy is instantaneously transferred from the shorter wavelength pump-light to the signal beam, using the non-linear properties of the material and taking advantage of the available high intensities. The transfer is instantaneous: there is no energy storage. To avoid damage and unwanted non-linear effects and to efficiently match and overlap with the length of the pump pulse, OPA can be combined with the abovementioned CPA technique, where pulses are stretched prior to amplification. These are called Optical Parametric Chirped Pulse Amplifiers (OPCPA). OPAs can cover a wide range of wavelengths from 300 nm to 4 μm. Most of the commercially available tunable wavelength sources are based on parametric oscillators or amplifiers. State-of-the-art OPCPA systems can generate 20 fs pulses with 1 J of energy and provide a focused intensity around 10^{20} W/cm², well exceeding the barrier for relativistic optics at 10^{18} W/cm² and giving the onset of non-linear effects and ionization.

The material is often chosen for its broad bandwidth or gain properties. Most efficient laser systems are working in the IR region for efficient pumping and energy storage, as well as for longer lifetimes. Applications often require light in the visible (experiments) or UV (injectors) ranges, which is achieved by converting the output wavelength, using non-linear crystals. Ultra-intense pulses can interact with non-linear or gaseous materials to extend their wavelength range from XUV to terahertz radiation. High order harmonics down to the XUV regime and with pulse durations inherently shorter than the drive pulse can be created, which opens up new application fields of attosecond science [10]. The scope of this paper does not allow for detailed expansion on this subject, but recommended reading is found in [11, 12].

Finally for some applications one might require treatment of the pulse after amplification, including spatial and longitudinal shaping. These include the use of adaptive optics, broadening

techniques in solid or gas, carrier-envelope stabilization for a few femtosecond pulses and programmable pulse trains. The specific techniques will be highlighted for applications with examples.

2 Lasers used in FELs, requirements, parameters and examples

FELs, based on LINACs and undulators, have been making their way to shorter wavelengths and a higher degree of coherence over the past decade, and at the 1 keV photon energy range they currently provide the brightest beams. This requires extremely high quality short electron bunches to be produced, with ultralow emittance.

Conventional lasers take their place all over the machine, as Fig. 7 illustrates. Fibre lasers and distribution systems are now routinely used in short-pulse FELs as the optical clock to provide the heart of the whole machine. These lasers can be locked to an external microwave crystal oscillator to achieve ultra-low reference noise and are distributed re-amplified and re-synchronized, achieving kilometre-long stabilized optical links [13, 14]. An overall stability of 10 fs can be routinely achieved in these systems. Photo-injection (PI) is used as the electron source, where electron bunches are produced through photo-emission from a cathode irradiated by a laser and are accelerated to a few MeV by the field present in the gun [15]. A laser heater is used to smooth out micro-bunching instabilities by inducing uncorrelated modulation to the bunch at a low energy [16, 17]. Lasers are an essential part of a FEL facility, not just by providing the primary electron source, but also by delivering ultra-short synchronized laser pulses for pump-probe measurements. As electron bunches are becoming shorter and shorter in the quest to produce XUV FEL pulses, conventional diagnostics devices are replaced by laser-based diagnostics, such as a laser wire to measure bunch cross-section [18], electro-optical bunch length and bunch arrival measurement [19–22]. These systems do not just provide superior accuracy in the femtosecond region, but are also non-invasive, by using laser fields for detection. Short wavelength FELs don't allow for amplification of the FEL pulse in cavities and therefore radiation is built up from self-amplification of spontaneous radiation from the undulators. As one seeds the undulators with a specific sub-harmonic wavelength, a higher gain and better beam quality can be reached in the same undulator length. Deep-UV and high-harmonic generation laser systems are used here for seeding the FEL [23–26].

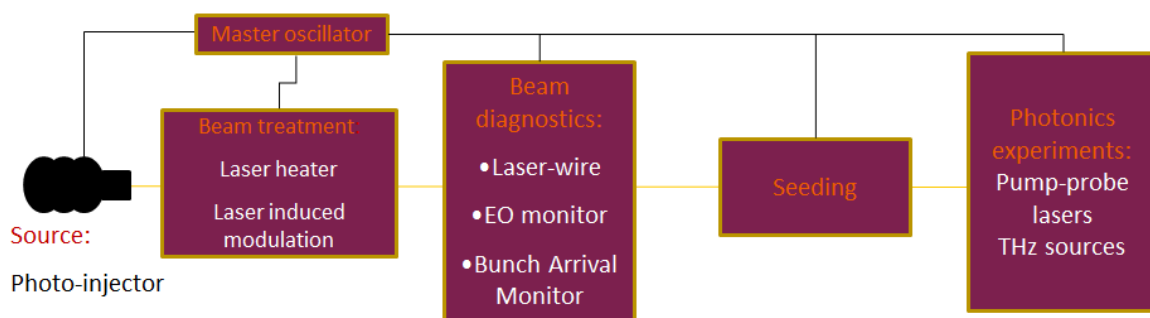


Fig. 7: Lasers used in FELs

As the stability and reliability of ultra-short pulse lasers is improved towards these applications, lasers are taking their own territory in accelerators and FELs by providing overall solutions for acceleration and beam production as well, aiming toward compact FELs.

All applications together require wavelengths from few a nanometres to terahertz, pulse energies from picojoules to multi-megajoules and pulse lengths from a single optical cycle to many picoseconds. Most of the time, additional flexibility is required, to cater for short- and long-pulse modes, and different pulse structures and wavelengths from the FEL. This calls for tunability in beam size, pulse length and sometimes also in the wavelength of the laser. It is not possible to cover all this within the scope of this

paper, but in the following sections some examples will be brought to illustrate the main parameters, requirements and challenges for each application.

2.1 Timing of the lasers

One of the requirements general to all lasers used in an FEL facility is the timing of the laser to the reference and to the entire machine. Figure 8 shows the schematic of the timing distribution over SwissFEL with all the time-of-arrival measurement and correction points. An optical master oscillator, based on an ytterbium fibre laser from OneFive, is operating at the low dispersion wavelength at 1550 nm [27]. The 200 fs long pulses at 142.8 MHz, which is the 21st sub-harmonic of the S-band RF, is distributed around the machine by stabilized fibre links. The RF distribution, the photo-injector laser [28], the laser-based beam arrival monitors and the experimental lasers are all synchronized to the clock pulses.

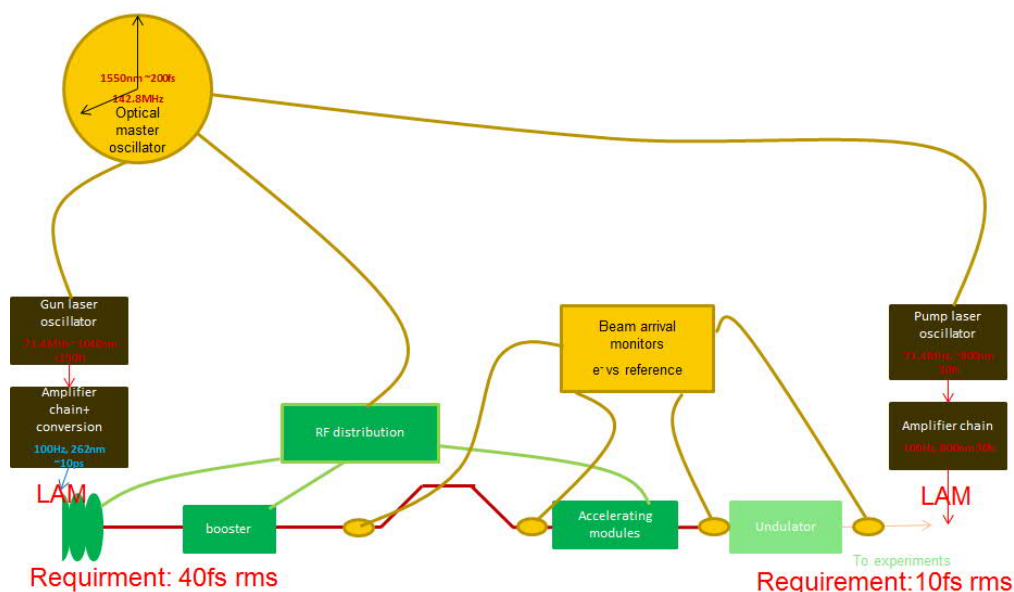


Fig. 8: Schematic of timing distribution for SwissFEL

At the injector the arrival time of the laser will determine the arrival time to the initial chicane and effect compression to produce shorter bunches. This in turn will influence the overall FEL lasing performance [29]. For the experimental lasers the users would ideally like to see their pump-probe experiment online, with the FEL and laser pulses arriving at a well-controlled delay at the femtosecond level. This problem is currently bridged by measuring the laser arrival time relative to the FEL at the experiment and binning the data afterwards for analysis. The ultimate aim is to apply a feedback system, which corrects the lasers' arrival over time. This is aided by locking the laser oscillator to the distributed reference. Large, ultra-short pulse laser systems include a long chain of optical components, however. As an example the Ti:Saph laser in the SwissFEL test facility [30, 31] includes 3 EO switches, 2 acousto-optical pulse shapers, 140 reflective surfaces and more than 7 crystals, and amounts to a total of 86 m of propagation path until it reaches the cathode for electron production. To reach the required 40 fs accuracy this length has to be stabilized to 12 μm accuracy. Mechanical vibrations, air-flow, electrical noise in the switches, thermal distortions and fluctuations, both in the cooling system for the crystals and in the environment, have detrimental effects on the arrival time. In a typical regenerative amplifier the expansion of the baseplate at 0.1°C change can induce drift at the 100 fs scale. Air temperature and pressure changes over long distances have the same effect. Therefore the direct control of the laser timing is necessary to maintain synchronicity with the rest of the system. Slow temperature-related drifts can easily be controlled with feed-forward systems, while fast variations related to vibrations are best passively tackled by design. Using kilohertz repetition rates and fast feedback, some of these noise

sources can also be damped. Laser- and beam-arrival monitors along the system are used to stabilize the subsystems. The optical clock becomes very useful, as direct comparison of these pulses with the laser pulses optically allows for measurements at 100 Hz.

2.2 Photo-injector lasers

In a photo-injector the electrons are produced by the photo-emission process. A photo-cathode is illuminated by laser pulses and the electrons are extracted by a high electric field inside the gun [15]. PI allows for approximately two orders of magnitude higher brightness than a conventional thermionic source, where electrons are produced by heat. Short pulses with 4D shaping have the potential to produce ultra-bright electron beams. Apart from the high particle beam quality achievable from these sources they also take advantage of the wide range of pulse length, repetition rates and pulse train structures that can be generated with laser oscillators, amplifiers and optical gating systems described in the previous section.

The main considerations for laser for photo-injectors include:

- i) Wavelength (tuned close to the work-function of the material):
 - Cs₂Te and Cu require UV ~260 nm;
 - GaAs needs IR and gives polarized electrons;
 - New type of alkaline cathodes, requiring visible light;
- ii) Timing:
 - The laser has to be synchronized to external reference/sub-harmonic of the RF;
 - Noise of the oscillator architecture, active elements need to support this;
- iii) Single pulse/burst mode to match machine operation:
 - Determines the chosen laser architecture (regenerative or multi-pass amplifier);
- iv) 3D–4D shaping to reduce emittance:
 - Beer-can/truncated Gaussian/ellipsoidal;
- v) Pulse length:
 - To mitigate space-charge effects at the gun;
 - To allow for shaping techniques;
- vi) Pulse energy:
 - Dependent on cathode choice/quantum efficiency and operational charge plus transport losses;
- vii) Reliability/reproducibility/stability:
 - Architecture used;
- viii) Running cost/service support.

When specifying a laser for a certain injector the cathode material will have a certain bandgap, which will determine the required laser wavelength. The relationship between the produced charge and the laser parameters can be described by the following simple equation

$$C [\text{nC}] = 8 \cdot QE [\%] \cdot W [\mu\text{J}] \cdot \lambda [\text{nm}] \quad (1)$$

where C is the produced charge in nC, QE is the quantum efficiency of the cathode as a percentage, W is the energy/micropulse in μJ and λ is the wavelength of the laser in nm (8 includes elementary charge, the Plank constant and speed of light).

Copper is usually used, when a charge below 1 pC is required for its robustness, long lifetime and easy production. This requires pulse energies in the tens of microjoule range. Alkaline cathodes, most typically Cs_2Te , are used for a higher charge at a cost of degrading efficiency and shorter lifetime, as well as more strict vacuum requirements. As the quantum efficiency is orders of magnitude higher, the laser energy can be in the nanojoule range, which also allows pulse trains to be delivered to the cathode. Both of these cathodes operate at a wavelength ~ 260 nm, which means fourth harmonic generation from the Nd and Yb doped lasers or third harmonic from a Ti:Saph laser. Producing and propagating UV light to the gun can be challenging due to losses or the conversion process and the degradation of the beam while propagating through air. Often, part of the beam transport has to be in vacuum.

As an example, Fig. 9 shows the SwissFEL photo-injector laser system [28]. The SwissFEL gun is a 2.5 cell S-band cavity, running at 100 Hz repetition rate. The peak acceleration is 120 MV/m and the required charge is up to 200 pC with the option to reduce down to a few picocoulombs for ultra-short FEL pulses. To maintain the space-charge conditions this in turn requires the scaling of the laser beam cross-section (0.1 nm to 0.27 mm) and pulse-length (4 ps to 10 ps) to match the charge. The normalized emittance requirement is 0.275/0.114 mm for the 100 pC and the 10 pC operational modes. To reach these values shaping of the laser pulse longitudinally and transversally to flat top is necessary. Both copper and Cs_2Te cathodes are used, therefore a large energy range has to be covered, up to 60 μJ . The stability is also crucial at the gun, as with single pulse operation the noise induced here cannot be reduced by feedback. The energy stability in the UV has to be below 0.5% RMS and the timing jitter below 40 fs. To reach these requirements the following architecture was chosen. The front-end oscillator is an ultra-low noise compact Yb fibre oscillator operating at 1040 nm. The oscillator is synchronized to the optical reference using RF locking to less than 30 fs integrated jitter. This can be further reduced by optical locking, which is planned for the future. The chirped pulse amplifier is a single-box regenerative amplifier with stabilized base-plates. The amplifier material is Yb:CaF₂, which allows short enough pulses for pulse-shaping purposes, but can still be directly diode-pumped. Part of the beam is used in the IR for the laser heater (described in the following section), while the rest of the output is converted to its fourth harmonic.

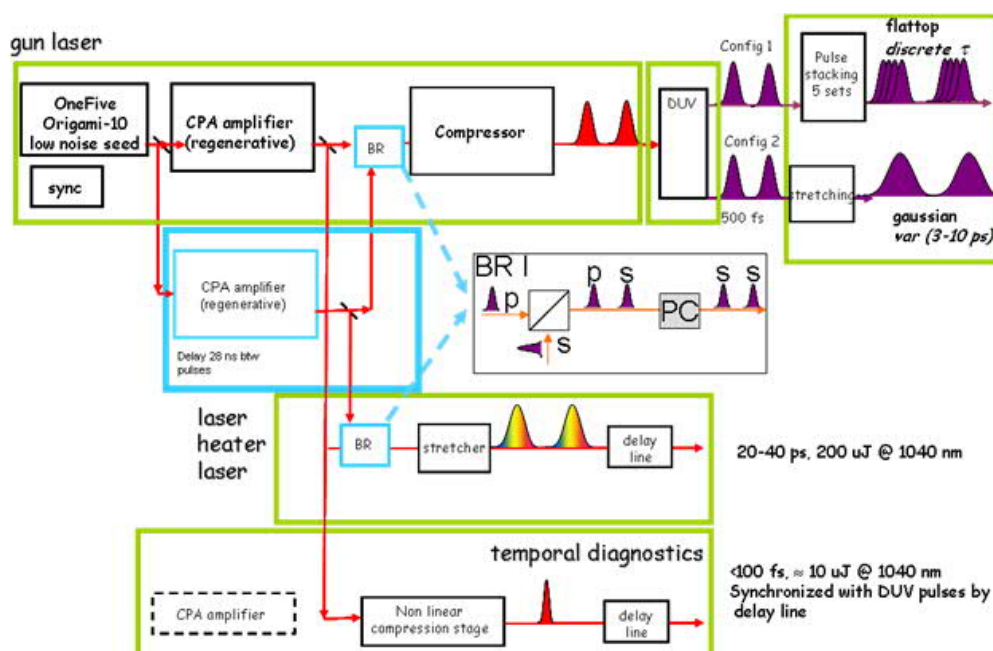


Fig. 9: The SwissFEL photo-injector laser system

Another example is the Nd:YLF system for FLASH [32] (Fig. 10). What makes this system more complicated is that there is a programmable train of pulses required at the cathode. This means that the single-box regenerative amplifier has to be replaced by multi-pass amplifiers, which run in a steady-state configuration to provide equal gain for each pulse in the train. After pre-amplification the pulses, which are amplified during the build-up of the gain, are rejected by an electro-optic switch (pulse picker) to produce a pulse train. All amplifiers are pumped by fibre-coupled pump diodes for accuracy, reliability and to remove the heat sources from the laser table.

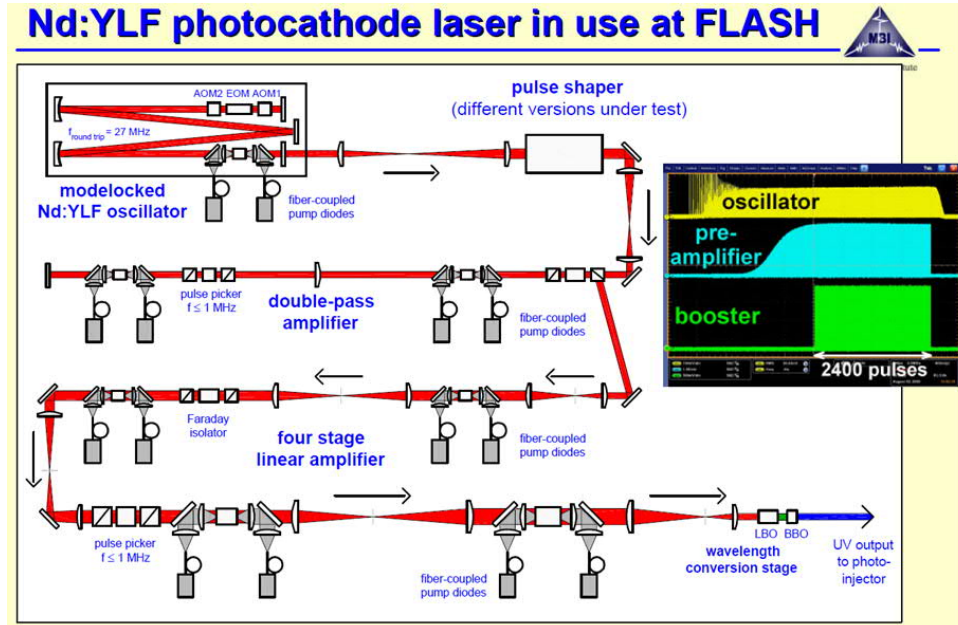


Fig. 10: Nd:YLF injector laser for FLASH

Pulse shaping is a very important aspect for achieving low emittance. Emittance at the gun is

$$\sigma = \sqrt{\sigma_{\text{spacecharge}}^2 + \sigma_{\text{thermal}}^2 + \sigma_{\text{RF}}^2} \quad (2)$$

The space-charge forces, which are determined by the electron distribution at the exit of the cathode, can be controlled by the laser pulse shape and the cathode response. Thermal emittance will be dependent on the work-function and the laser wavelength. When approaching the bandgap of the cathode material with the wavelength, lower thermal emittance can be achieved, but at the cost of reduced QE . The RF field will also make a contribution to the emittance. This has been demonstrated in the SwissFEL Tests Injector, where a Ti:Saph laser with tunable wavelength was converted to its third harmonic to illuminate the cathode. By reducing the wavelength from 267.5 nm to 260 nm the thermal emittance has increased from 584 nm/mm to 626 nm/mm and QE increased by ~50% [33]. In a linac with proper focusing, emittance due to linear space-charge force can always be compensated. Hence, the idea that the laser should be shaped to be flat top both in space and time. This is applied in many working machines, such as LCLS, FLASH, SPARC, PITZ and SwissFEL. More information on the techniques used can be found in [34]. A great deal of effort was invested to produce such flat top pulses in time. While the spatial distribution can be achieved by simply aperturing the laser beam and projecting this plane to the cathode, the temporal distribution is harder to achieve. Fourier transformation shows that when sharp edges are created in time they require infinite frequencies, which is not possible in the practical world. Gaussian ‘wings’ are therefore accepted at the rising and falling edges of the pulse. A simple technique applied for UV pulse shaping is a passive, so-called pulse-stacking system, where the pulses are propagated through birefringent crystals, which induce replica pulses with a certain delay. The sum of the pulses then gives a quasi-flat top distribution in time. This, however, suffers from ripples

on the top of the pulse. Care needs to be taken that the frequency of the modulation caused by the finite number of pulses and interference between them is not enhancing micro-bunching instabilities in the machine. The technique was further developed at BMI, where the shaping takes place in the IR, directly after the oscillator and the crystals are temperature-controlled to maintain, and also to actively program, the pulse shape [35]. A new approach to shaping the laser pulse into a ‘rugby ball’ provides even better emittance on paper, but the production and propagation of such a beam in the UV is still challenging. Tests were performed in PITZ in this direction [36]. Finally, Table 2 gives a summary of the different types of photo-injector laser currently in use with FELs [37–49].

Table 2: Photo-injector lasers around the world

	ELSA	FLASH (FEL)	TESLA	LCLS	ELETT RA	European XFEL	SwissFEL
Cathode	K ₂ CSSb	Cs ₂ Te	Cs ₂ Te	Cu	Cu	Cs ₂ Te	Cs ₂ Te/Cu
Wavelength on cathode [nm]	532	262	263	253	261	262	260
Pulse length on cathode [ps]	30	4.4	20 square	3 to 20 square	6 to 15	6	4 to 10 square
Material	Nd:YAG	Nd:YLF	Nd:YLF; Nd:glass	Ti:Saph	Ti:Saph	Nd:YLF	Yb:CaF ₂
Harmonic	2nd	4th	3rd and mixing	3rd	3rd	4th	4th
Macropulse rep. rate [Hz]	1	≤10	10	30 to 120	≤50	1 to 5	≤100
Micropulse rep. rate [MHz]	14.4	27	1	NA	NA	1500	NA
Pulse train length	150 μs	≤800 μs	800 μs	NA	NA	1.3 μs	2 pulses
Pumping [†]	FL	D, FL	FL	L	L	L	D
Energy/pulse IR	10 μJ	300 μJ	200 μJ	25 mJ	15 mJ	5 μJ	2 mJ
Macro-pulse stability	3%	–	3% (<10%)	–	0.8%	1.5% to 3% (<0.5% in IR)	Na
Micro-pulse stability	?	1% to 2%	(<5%)	–	–	–	0.7%

[†]FL, flashlamp; D, diode; L, laser.

2.3 Laser heater

Following the order of the lasers found in the machine, the next is the laser heater [16, 17]. If short pulses are generated in an RF gun with small momentum spread, due to ripples and oscillations in the pulse and their interaction with the accelerating field, the pulses can suffer from so-called micro-bunching instabilities. The laser heater superimposes a polarized laser beam and the electron beam in a properly tuned undulator. This produces a momentum modulation which smeared out in a chicane to obtain the desired momentum spread increase. To match the bunch length and the physical size of the undulator the lasers used for the laser heater are working in the IR range (~0.8 μm to 1 μm). The pulse length needs to be in the tens of picoseconds Gaussian, with cross-section to match or overfill the size of the electron beam in the undulator. The energy required is ~100 μJ. The pulse structure matches the

electron beam structure. Usually they can rely on the fundamental radiation from the gun laser system. This has the advantage of the lasers being inherently locked together in timing and having the same pulse structure. As the heater is usually a few tens of metres from the gun, propagating the beam to it from the gun laser room is possible, but sometimes requires active beam-steering and stabilization to get through the undulator.

2.4 Experimental lasers

Laser used for experiments are the most sophisticated and versatile as they have to cover many different applications. Biological studies require visible and ultraviolet light, femtosecond chemistry relies on 800 nm Ti:Saph lasers, molecular studies need mid-infrared radiation, while magnetization studies reach into the terahertz range.

General requirements are synchronizability to the machine, matching of the pulse structure of the FEL, femtosecond accuracy and scanning capability and pulse length at least as short as the FEL's. There are also resonance experiments where wavelength tuning, although with longer pulses, is a requirement.

I bring here as an example the European XFEL laser [50], used for pump-probe and molecular alignment studies (Fig. 11). Because of the burst mode operation of the machine, the laser has been developed specially for this machine. The intra-pulse repetition rate is up to 4.5 MHz with up to 2700 pulses in each burst, delivered at up to 10 Hz repetition rate. At 800 nm, 15 fs to 300 fs long pulses are required with arbitrary pulse pattern selection. The pulses are then converted to different wavelengths. This is all achieved by a fibre–solid-state and OPA system. A Yb fibre oscillator, which is synchronized to the external reference, is further amplified in a CPA system before splitting part of the beam to further amplify it in a 400 W InnoSlab amplifier and 5 kW InnoSlab booster. The pulses here are selected by an electro-optical modulator and compressed from 400 ps to 800 fs. This part of the beam is converted to its second harmonic and is used to pump the OPA stages. A 2 μJ fraction of the 1030 nm booster output is compressed down to 300 fs. This high intensity allows for supercontinuum generation to generate a wider range of wavelengths for the OPA stages, which can be tuned by the crystal angle, as they work in a non-collinear arrangement. The final system delivers up to 2 mJ pulses.

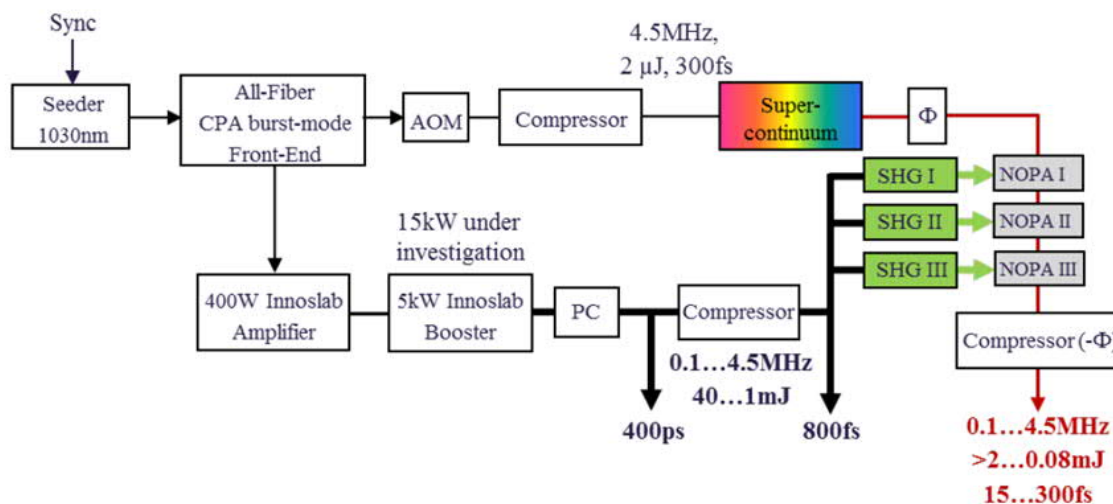


Fig. 11: The experimental laser of the European XFEL

Other experiments around the XFEL require less unique configurations. For the high intensity (HI) and high energy (HE) stations a commercial TW class Ti:Saph system and a kilojoule nanosecond laser are used, respectively.

Another example from SwissFEL is shown in Fig. 12. The core laser system is a commercial Ti:Saph system from Coherent Inc., delivering 20 mJ pulses compressed to <30 fs at 100 Hz. Two identical lasers will be used to ensure redundancy in the case of failure. The lasers will be housed in the room above the experimental stations. The local installation in the experimental station includes a Light Conversion Ltd OPA, delivering pulses from 1.1 mm to 15 mm with ~1 mJ to 10 mJ of energy, respectively. The pulse length is below 100 fs. The output of the OPA will also be used to pump organic crystals for terahertz pulse generation with 1 THz to 10 THz of >1 MV/cm electric field strength in ~10 μ J single-cycle pulses. For pulses shorter than the standard 30 fs output of the main laser system, hollow core fibre, kagome fibre and halogen gas chambers are being investigated. The hall also houses the laser arrival monitor and the THz streak camera, to ensure accurate timing between the laser and the X-rays.

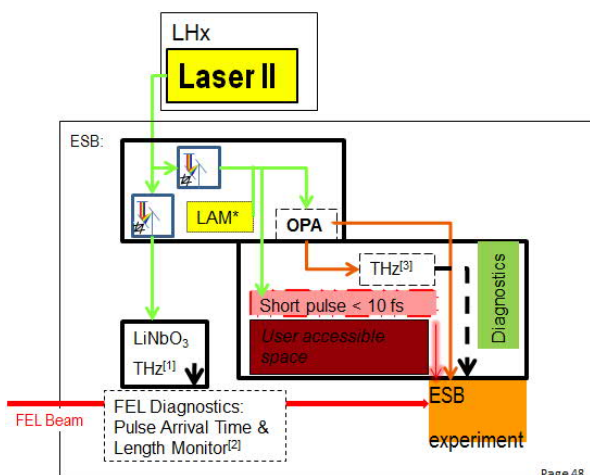


Fig. 12: The laser in the experimental hall of SwissFEL

Finally, mention is made of the requirements for infrared FELs: the FELBE facility is used as an example [52]. For tuneability a range of Ti:Saph lasers are used in conjunction with parametric oscillators and amplifiers, as well as different frequency stages. For the low energy pulses the repetition rates are at 78 MHz, and pulse energies range from 4 nJ to 150 nJ with pulse lengths from 15 fs to 100 fs. Regenerative amplifiers provide higher pulse energies above 200 μ J with 1 kHz repetition rate. In addition, the laser systems are suitable for generating broadband terahertz pulses, which can be used for probing the dynamics excited with FEL pulses (FEL-pump – broadband terahertz probe). All lasers can be synchronized to the FEL.

2.5 Seeding laser

As radiation in an X-ray FEL builds up from the initial noise, there is a lack of temporal coherence in the SASE beam. This can be helped by seeding the FEL with a wavelength that is tuned to a sub-harmonic of the FEL [23–26]. Pulses should also be short and therefore the application of high harmonics from lasers is a natural choice. This way the input signal, the so-called seed, is coherently amplified in the FEL. Seeding was demonstrated at FERMI@Elettra down to 10 nm wavelength.

The advantages of such seeding arrangement are:

- Very high peak flux and higher 6D brightness than with SASE;
- Temporal and transverse coherence of the FEL pulse;
- Control of the time duration, polarization, wavelength and bandwidth of the FEL pulse;
- Inherent synchronization of the FEL pulse to the seed laser, which is also often used for experiments;

- Reduction in undulator length needed to achieve saturation as compared to starting from noise as in SASE FELs.

To achieve efficient FEL seeding a spatial overlap between the electron and laser beams is required, and therefore good pointing stability from the optical laser is needed. The harmonic parameters, such as energy, chirp and wavelength, need to be within the tolerance of the undulator. Temporal overlap between the laser and the electron beam needs to be maintained and the jitter has to be below the sigma bunch length for stable output.

A White Paper was written by the ICFA-ICUIL Joint Task Force to identify high power laser technological needs for accelerators [54]. It was shown, that to reach the required energy levels for seeding at the 30 eV to 0.25 keV range, tens of μJ energies in 100 kHz bursts would be needed. This requires a beast of a 100 GW Ti:Saph laser with a pulse length at 10 fs. Either of these parameters on its own is a challenge. For hard X-rays, similar energy and power levels are necessary, but at a different wavelength, which allows the use of diode-pumped solid-state lasers in conjunction with OPCPA. To develop such lasers at 100 GW levels, however, still requires R&D.

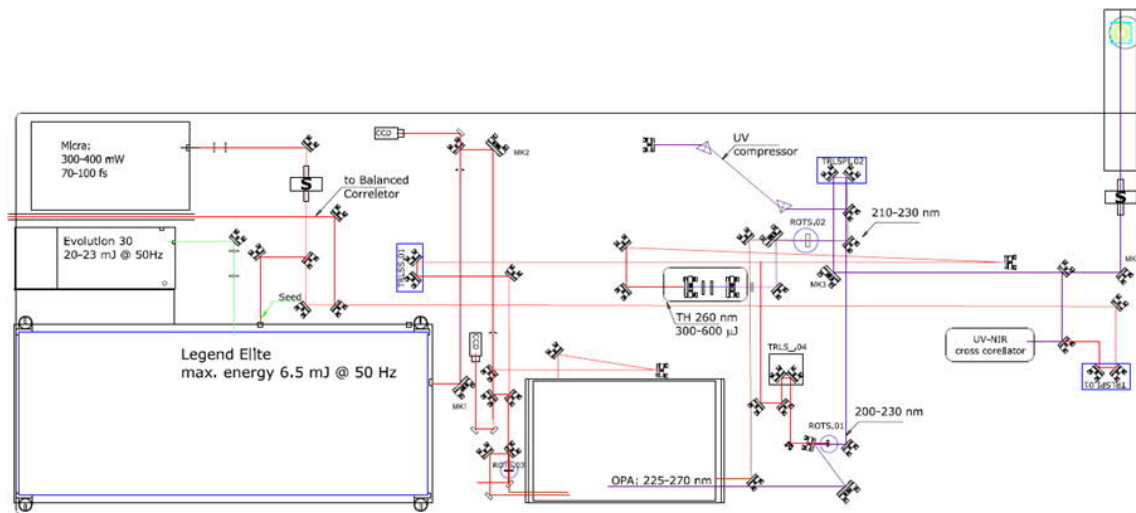


Fig. 13: Seed laser at Fermi@ELETTRA

Figure 13 shows the layout of the Fermi seeding laser for a High Gain Harmonic Generation (HG) scheme [55]. It is possible to reach the wavelengths required here with conventional harmonic generation crystals (>200 nm). The system is delivered by Coherent Inc. The Micra Ti:Saph oscillator delivers <100 fs pulses with 400 mW average power. An Evolution 23 mJ green laser provides the pumping at 50 Hz for the amplifier, where a single pulse is recirculated and 6.5 mJ is produced in the infrared. A standard third harmonic generation stage delivers 260 nm, while a tunable OPA gives the seed for the variable UV output stage. Table 3 summarizes the required and achieved parameters.

Table 3: Fermi@ELETTRA seed laser parameter requirements, with the achieved values in brackets

Parameter	Tunable UV	Fixed UV
Tunability range [nm]	210 to 280 (230 to 260)	261 197
Peak power [MW]	100	>400
Pulse duration [fs]	100 (180)	<150 (150 to 500)
Pulse energy stability [RMS, 5000 shots]	$<4\%$	$<2\%$
Timing jitter RMS [fs]	<50 (100)	<50 (100)
Spot in undulator $1/e^2$ [mm]	1	1 to 1.2
Wavelength stability	10^{-4}	$<10^{-4}$
Beam quality $[M^2]$	<2	<1.5

To seed hard X-rays shorter wavelengths are necessary: 1 nm to 20 nm. Here, high harmonic generation from the laser is used. At high laser intensities the laser field is strong enough to suppress the coulomb barrier and therefore an electron is able to tunnel out of the atom. The laser's electric field then accelerates this electron in a half-cycle. The electron can then be steered back by the opposite electric field from the laser and recombine with the parent ion, while emitting a photon at a higher energy. The high harmonic radiation forms a 'comb', where the energies are separated by half of the drive-laser period, due to the acceleration and recombination process. Such a comb structure, when Fourier-transformed, corresponds to an attosecond pulse train in the time domain. At sFLASH such a scheme was used to seed the FEL, using an off-the-shelf laser system at 800 nm, with 20 mJ laser energy and 35 fs pulses. HHG targets usually consist of a noble gas and a guiding structure.

Most FELs are now aiming for self-seeding arrangements, where a monochromator is used between subsequent undulators and the residual beam is used for seeding [56, 57]. The process, however, is much more lossy and the output after the monochromator is much more unstable than a laser seed.

2.6 Diagnostics lasers

The electro-magnetic field of the laser is used often as a tool for diagnostics due to its non-invasive nature. Lasers are used to measure beam size, electron bunch length and time of arrival as well as to characterize the final photon beam of the FEL. The following section will not give an exhaustive summary, but more of a taster on how lasers can be used for diagnostics. The references should be studied in more detail for each application.

A laser wire scanner is used at CAEP FEL to measure the transverse beam size of the electron beam at 250 keV [18]. The energy of the beam in this particular case is very low and therefore a non-invasive solution is very attractive. The bunch length is 15 ps and the repetition rate is very high at ~54 MHz, with a high bunch charge of 100 pC. The laser is propagated perpendicularly to the beam and is at 5 ps length to ensure accurate timing overlap. The focusing arrangement is chosen so that the Rayleigh range of the laser beam overlaps with the longitudinal size of the electron bunch. As only about 55.4 nJ energy is required an oscillator and a booster amplifier are sufficient. The laser is operating at 532 nm, using the second harmonic light of a neodymium laser. The interaction is based on Compton scattering.

Another well-established application is electro-topical bunch length and arrival time measurement [19–22]. All of these devices take advantage of the coulomb field generated by the electron beam. When using specific electro-optical crystals, which change their properties due to this field, one can map the properties of the electron beam in time by encoding the information into a short laser pulse passing through the crystal. The encoding can take place in the spectral domain, making the readout simple. For scanning methods the coincidence of the laser and the electron-pulse can be read out by a photodiode, while for single shot measurements a CCD is used to map the spectrum. Spatial encoding is also possible, though the imaging limits the resolution and the electron beam has to pass through the crystal. Temporal encoding mixes a reference pulse with the spectrally encoded pulse to achieve tens of femtoseconds resolution. Most methods are limited by the crystal size, as the signal strength is proportional to this, but the encoding is smeared out when thicker crystals are used. Relatively low energy but broadband pulses are needed, with a pulse structure matching the FEL's Ti:Saph laser, so pulses that are used for experiments can be split off for this purpose, or from fibre lasers with a broadening stage.

Beam arrival monitors are very important to keep the whole machine, often spread over several hundred metres, in synchronization. They use RF antennae to pick up the signal from the electron beam and use this signal with appropriate attenuation to drive an electro-optical modulator. The signal to be modulated is the optical pulsed reference. The signal, which is proportional to the relative delay between the optical reference and the pickup signal, is read out by a photodiode. Here 20 fs resolution can be achieved.

A THz streak camera is used to measure the relative timing between the X-ray and the pump laser pulses, as well as to characterize the FEL pulse length [58–60]. The technique has been adapted from the attosecond world, where an electric field of a few cycles of IR pulses are used to sweep the electrons [61], which are generated by ionization from the X-ray pulses, as shown in Fig. 14. The linear part of the laser’s electric field has to match the pulse length. As FEL pulses are longer, one has to move to longer laser wavelengths, hence to terahertz pulses. The other requirement is the field strength, which has to be strong enough to deviate the electrons by an amount that is detectable by a time-of-flight device. The challenge also lies in the initial temporal and spatial overlap of the terahertz and X-ray pulses, both propagating in vacuum. This technique is also used for the AMO at LCLS.

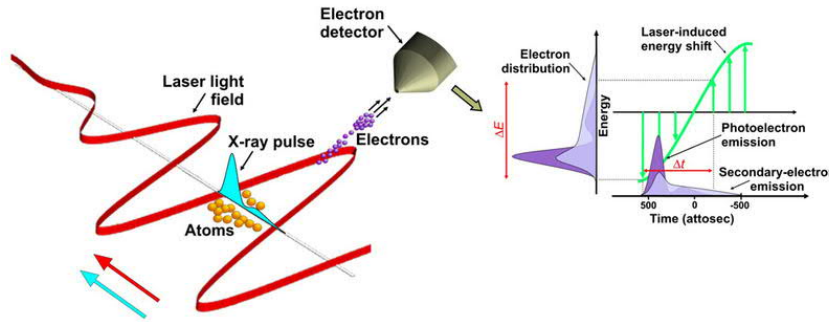


Fig. 14: A schematic of the operation of a THz streak camera

The laser system at FERMI@Elettra is a fine example of how a laser can be utilized for most tasks in the FEL. The same laser is used for seeding and experiments as well as for the time-of-arrival measurements. The long optical passes are actively stabilized to keep the synchronization between the different parts of the machine.

3 The future of lasers in FEL

Figure 15 shows the state-of-the-art for X-ray short pulse sources based on lasers and on FELs. With new projects, such as Extreme Light Infrastructure (ELI) [63] and Berkeley Lab Laser Accelerator (BELLA) [64] the photon energy gap between the two types of sources is closing. Both of these facilities utilize a petawatt laser, giving multiple tens of joules of laser energy in a single pulse at 1 Hz. The aim is to produce accelerating gradients reaching 100 GV/m by laser plasma acceleration. Eventually, robust fibre technology developed for telecommunications could provide large numbers of lasers locked together to reach joules of energy to drive laser plasma accelerators as well.

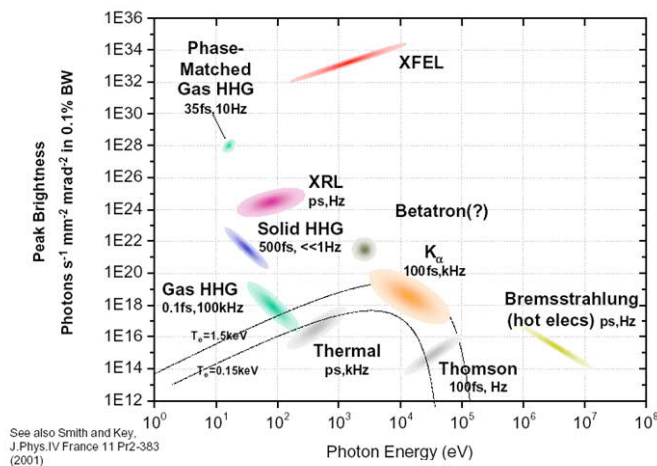


Fig. 15: Short pulse X-ray sources

The Advanced Proton Driven Plasma Wakefield Acceleration Experiment (AWAKE) project at CERN is aiming to combine the best of both accelerator and laser technology and accelerate an electron beam produced by a photo-injector using proton-driven plasma wakefield acceleration. The plasma is produced by a laser and the modulation, which drives the acceleration, is induced by self-modulation instabilities from the proton beam. The aim is to create GV/m accelerating strengths.

Scaling to higher repetition rates on the laser side has already been achieved, and commercial high pulse energy ultra-short pulse laser systems at a few kilohertz are already available on the market, while similar scaling for high power RF distribution is not clear. In conjunction with laser wakefield acceleration techniques, these lasers can provide tabletop X-ray sources for universities, small laboratories and medical treatment centres. I am certainly looking forward to reading the school notes in ten years' time on the same subject.

References

- [1] A. Siegman, *Lasers* (University Science Books, 1986).
- [2] Gould and R. Gordon, The LASER, light amplification by stimulated emission of radiation, Ann Arbor Conference on Optical Pumping, Michigan, 1959, Eds. P.A. Franken and R.H. Sands. OCLC 02460155, p. 128.
- [3] Einstein A, *Verh. Dsch. Phys. Ges.* **18** (1916) 318.
- [4] K.R. Spring, T.J. Fellers and M.W. Davidson, Introduction to lasers, <http://www.olympusmicro.com/primer/techniques/confocal/laserintro.html> (Olympus, 2012).
- [5] W. Koechner, *Solid-State Laser Engineering* (Springer-Verlag, New York, 2006).
- [6] P. Polynkin, A. Polynkin, D. Panasenko, N. Peyghambarian, M. Mansuripur and J. Moloney, *Opt. Lett.* **31**(5) (2006) 592. <https://doi.org/10.1364/OL.31.000592>
- [7] D. Strickland and G. Mourou, *Opt. Commun.* **56**(3) (1985) 219. [https://doi.org/10.1016/0030-4018\(85\)90120-8](https://doi.org/10.1016/0030-4018(85)90120-8)
- [8] D. Strickland, P. Bado, M. Pessot and G. Mourou, *IEEE J. Quant. Electr.* **24**(2) (1988) 398. <https://doi.org/10.1109/3.137>
- [9] A. Doyuran *et al.*, *NIMA in Phys. Res. A* **528**(1–2) (2004) 467. <https://doi.org/10.1016/j.nima.2004.04.133>
- [10] F. Krausz and M. Ivanov, *Rev. Mod. Phys.* **81**(1) (2009) 163. <https://doi.org/10.1103/RevModPhys.81.163>
- [11] Sutherland: *Handbook of Nonlinear Optics* (CRC Press).
- [12] J.-C. Diels and W. Rudolph, *Ultrashort Laser Pulse Phenomena* (Elsevier, Amsterdam, 2006).
- [13] X. Chen *et al.*, *Sci. Rep* **5** (2015) 18343. <https://doi.org/10.1038/srep18343>
- [14] B. Ning *et al.*, *Sci. Rep.* **4** (2014) 5109. <https://doi.org/10.1038/srep05109>
- [15] R.L. Sheffield *et al.*, *Science* **274**(5285) (1996) 236. <https://doi.org/10.1126/science.274.5285.236>
- [16] E.L. Saldin, E.A. Schneidmiller and M.V. Yurkov, *NIM A* **490**(1–2) (2002) 1. [https://doi.org/10.1016/S0168-9002\(02\)00905-1](https://doi.org/10.1016/S0168-9002(02)00905-1)
- [17] Z. Huang *et al.*, *Phys. Rev. ST Accel. Beams* **7**(7) (2004) 074401. <https://doi.org/10.1103/PhysRevSTAB.7.074401>
- [18] A. Bosco *et al.*, *Nucl. Instrum. Meth. A* **592**(3) (2008) 162. <https://doi.org/10.1016/j.nima.2008.04.012>
- [19] I. Wilke, A.M. MacLeod, W.A. Gillespie, G. Berden, G.M.H. Knippels and A.F.G. van der Meer, *Phys. Rev. Lett.* **88**(12) (2002) 124801. <https://doi.org/10.1103/PhysRevLett.88.124801>
- [20] A.L. Cavalieri *et al.*, *PRL* **94**(11) (2005) 114801. <https://doi.org/10.1103/PhysRevLett.94.114801>

- [21] S.P Jamison *et al.*, *Opt. Lett.* **28**(18) (2003) 1710. <https://doi.org/10.1364/OL.28.001710>
- [22] J. van Tilborg *et al.*, *Opt. Lett.* **32**(3) (2007) 313. <https://doi.org/10.1364/OL.32.000313>
- [23] M. Ferray *et al.*, *J. Phys. B At. Mol. Opt. Phys.* **21**(3) (1988) L31. <https://doi.org/10.1088/0953-4075/21/3/001>
- [24] G. Lambert *et al.*, *Nat. Phys. Lett.* **295** (2008).
- [25] L. Gianessi *et al.*, *Nucl. Inst. & Meth. A* **594** (2008) 132. <https://doi.org/10.1016/j.nima.2008.04.073>
- [26] C. Lechner *et al.*, First direct seeding at 38 nm, Proc. FEL Conf., Nara, 2012.
- [27] Ultra low timing jitter performance & characterization of Origami femtosecond laser series, P/N 09-001 (Onefive GmbH, Regensburg, 2016) http://www.onefive.com/uploads/ultra_low-noise_whitepaper_onefive_v9_rev1.2.pdf.
- [28] A. Trisorio *et al.*, New concept for the SwissFEL Gun laser, Proc. FEL, New York, 2013.
- [29] B. Beutner and S. Reiche, Proc. FEL, Malmö, Sweden, 2010, WEPB17.
- [30] M.C. Divall, A. Romann, P. Mutter, S. Hunziker and C.P. Hauri, Laser arrival measurement tools for SwissFEL, Proc. SPIE 9512, Advances in X-ray Free-Electron Lasers Instrumentation III, Prague, 2015, 95121T (SPIE, 2015). <https://doi.org/10.1117/12.2179016>
- [31] M.C. Divall, P. Mutter, E.J. Divall and C.P. Hauri, *Opt. Express* **23**(23) (2015) 29929. <https://doi.org/10.1364/OE.23.029929>
- [32] I. Will, H.I. Templin, S. Schreiber and W. Sandner, *Opt. Express* **19**(24) (2011) 23770. <https://doi.org/10.1364/OE.19.023770>
- [33] M. C. Divall, E. Prat, S. Bettoni, C. Vicario, A. Trisorio, T. Schietinger and C. P. Hauri, *Phys. Rev. ST Accel. Beams* **18**(3) (2015) 033401. <https://doi.org/10.1103/PhysRevSTAB.18.033401>
- [34] M. Divall, Beam shaping, LA3NET School, Caen, 2012 (Paul Scherrer Institut, 2012) https://indico.cern.ch/event/177701/contributions/1441170/attachments/232573/325458/beam_shaping_Marta_Divall.pdf.
- [35] I. Will and G. Klemz, *Opt. Express* **16**(19) (2008) 14922. <https://doi.org/10.1364/OE.16.014922>
- [36] M. Bakr , G. Vashchenko, M. Khojayan, M. Krasilnikov and F. Stephan, Proc. FEL2015, Daejeon, 2015, TUP065 (2015).
- [37] A. Gallo *et al.*, Laser and RF synchronization measurements at SPARC, Proc PAC07, Albuquerque, 2007 (2007). <https://doi.org/10.1109/PAC.2007.4440959>
- [38] T.J. Maxwell *et al.*, Synchronization and jitter studies of the titanium-sapphire laser at the A0 photoinjector, Proc PAC11, New York, 2011, MOP285 (2011).
- [39] H. Qian *et al.*, Timing jitter characterization at the NSLS SDL, Internal note for Brookhaven Science Associates BNL-82276-2009-CP (2009).
- [40] N. Cutic *et al.*, On-line arrival time and jitter measurements using electro-optical spectral decoding, Proc. FEL2010, Malmoe, 2010, THOA4, (2010).
- [41] Schulz *et al.*, Precision synchronization of the Flash Photoinjector Laser, IPAC10, Kyoto, 2010, WEPWB076 (2010).
- [42] A. Azima *et al.*, Jitter reduced pump-probe experiments. Proc of DIPAC 2007, Venice, Italy.
- [43] A. Sakumi *et al.*, Synchronization between laser and electron beam at photocathode RF gun, Proc PAC05, Knoxville, 2015 (2005).
- [44] J.W. Bähr *et al.*, BIW10, TUPSM103 (2010).
- [45] M. Krasilnikov *et al.*, DESY-M-04-03U (2004).
- [46] V. Le Flanchec, J.-P. Blésès, S. Striby and J.-P. Laget, *Appl. Opt.* **36**(33) (1997) 8541. <https://doi.org/10.1364/AO.36.008541>
- [47] A.R. Fry *et al.*, Proc. PAC1997, 4w022 (1997).

- [48] M. Danailov *et al.*, Proc. International FEL Conf. 2007.
- [49] P. Singalotti *et al.*, Ultrafast laser synchronization at the FERMI@Elettra FEL, Proc. SPIE Vol. 8778 87780Q (2013). <https://doi.org/10.1117/12.2020488>
- [50] M. Lederer, Laser systems for science instruments, European XFEL Users' Meeting, Hamburg, 2017, http://www.xfel.eu/sites/site_xfel-gmbh/content/e63594/e65073/e275358/e278336/04LasersystemsforscienceinstrumentsML_eng.pdf.
- [51] C. Erny and C.P. Hauri, *J. Synchrotron Radiat.* **23** (2016) 1143. <https://doi.org/10.1107/S1600577516012595>
- [52] M. Helm and P. Michel, *Notiziario Neutroni E Luce Di Sincrotrone* **11** (2006) 33. http://statistics.roma2.infn.it/~notiziario/2006/11_2_06/pag33.pdf
- [53] E. Allaria *et al.*, *New J. Phys.* **14** (2012) 11300. <https://doi.org/10.1088/1367-2630/14/11/113009>
- [54] W. Leemans, High power laser technology for accelerators, White Paper of the ICFA-ICUIL Joint Task Force.
- [55] FERMI. Elettra and FERMI lightsources. 2013-10-24. <http://www.elettra.trieste.it/lightsources/fermi.html>.
- [56] J. Amann *et al.*, *Nat. Photon.* **6** (2012) 693. <https://doi.org/10.1038/nphoton.2012.180>
- [57] I. Gorgisyan, P.N. Juranic, R. Ischebeck, A. Stepanov, V. Schlott, C. Pradervand, L. Patthey, M. Radovic, R. Abela, C. P. Hauri, B. Monoszlai, R. Ivanov, P. Peier, J. Liu, T. Togashi, S. Owada, K. Ogawa, T. Katayama, M. Yabashi and L. Rivkin, The new design of the THz streak camera at PSI, Proc. SPIE 9512, Advances in X-ray Free-Electron Lasers Instrumentation III, 95120D (SPIE, 2015). <https://doi.org/10.1117/12.2182204>
- [58] I. Grguras *et al.*, *Nat. Photon.* **6** (2012) 852. <https://doi.org/10.1038/nphoton.2012.276>
- [59] U. Fröhling *et al.*, *Nat. Photon.* **3** (2009) 353. <https://doi.org/10.1038/nphoton.2009.160>
- [60] P. Juranic *et al.*, *JINST* **9** (2014) P03006. <https://doi.org/10.1088/1748-0221/9/03/P03006>
- [61] M. Hentschel *et al.*, *Nature* **414** (2001) 509. <https://doi.org/10.1038/35107000>
- [62] Helml *et al.*, *Nat. Photon.* **8** (2014) 950. <https://doi.org/10.1038/nphoton.2014.278>
- [63] D. Jaroszynski, Ultra-short duration electron and radiation pulses from the laser-plasma wakefield accelerator, ELI-NP, 2015, http://www.eli-np.ro/2015-summer-school/presentations/24.09/Jaroszynski_ELI-NP_ss.pdf
- [64] BELLA, Berkeley Lab, <http://bella.lbl.gov/>.
- [65] Advanced wakefield experiment, (2013) <http://awake.web.cern.ch/awake/>